THE JOURNAL OF PHYSICAL CHEMISTRY Letters

PERSPECTIVE

pubs.acs.org/JPCL

Materials Challenges and Opportunities of Lithium Ion Batteries

Arumugam Manthiram*

Electrochemical Energy Laboratory & Materials Science and Engineering Program, The University of Texas at Austin Austin, Texas 78712, United States

ABSTRACT Lithium ion batteries have revolutionized the portable electronics market, and they are being intensively pursued now for transportation and stationary storage of renewable energies like solar and wind. The success of lithium ion technology for the latter applications will depend largely on the cost, safety, cycle life, energy, and power, which are in turn controlled by the component materials used. Accordingly, this Perspective focuses on the challenges and prospects associated with the electrode materials. Specifically, the issues associated with high-voltage and high-capacity cathodes as well as high-capacity anodes and the approaches to overcome them are presented.

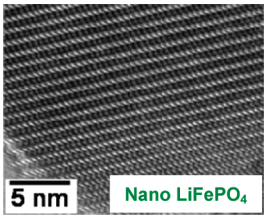

Lithium ion batteries have aided the portable electronics revolution during the past 2 decades because they store much higher energy per unit weight or volume compared to other rechargeable battery systems. The higher energy density is due to our ability to achieve high voltages (3−5 V per cell) due to the use of nonaqueous electrolytes along with high capacity values compared to <2 V normally realized with aqueous electrolyte-based battery systems. Due to the higher energy densities, lithium ion batteries are now being intensively pursued for transportation applications, including hybrid electric vehicles (HEV), plug-in hybrid electric vehicles (PHEV), and electric vehicles (EV). They are also being seriously considered for the efficient storage and utilization of intermittent renewable energies like solar and wind. Renewable energies will not have the anticipated impact unless we find an efficient way to store and use the electricity produced by them; batteries are an attractive option for this. Cost, safety, cycle life, energy, and power are some of the major issues in successfully adopting the lithium ion technology for transportation and stationary electrical energy storage, and these parameters are in turn linked to the electrode (anode and cathode) and electrolyte materials used.[1] This Perspective focuses on the challenges and prospects associated with electrode materials for next-generation lithium ion batteries.

Renewable energies will not have the anticipated impact unless we find an efficient way to store and use the electricity produced by them; batteries are an attractive option for this.

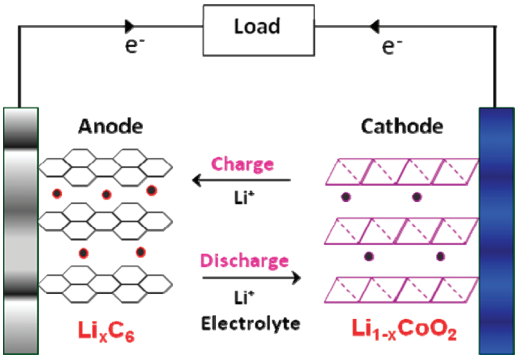

Figure 1. Illustration of the charge/discharge process involved in a lithium ion cell consisting of graphite as the anode and layered $LiCoO_2$ as the cathode.

Electrode Materials. Figure 1 illustrates the operating principles involved in a lithium ion cell. Basically, the lithium ions are shuttled between two insertion host electrodes (anode and cathode) during the charge−discharge process. Table 1 provides an overview of the major class of lithium insertion electrode materials that are currently in play. Each system in Table 1 has its own advantages and disadvantages, which often dictate their application areas. For example, the layered $LiCoO_2$ cathode has revolutionized portable electronics like cell phones and laptop computers, but the high cost, toxicity, chemical instability at deep charge, and safety concerns associated with $LiCoO_2$ prevent its use for transportation and stationary storage applications. The chemical instability and the consequential safety concerns of $LiCoO_2$ arise from an overlap of the $Co^{3+/4+}$:3d band with the top of the O^{2-}:2p band, which also limits the practical capacity of $Li_{1-x}CoO_2$

Received Date: November 12, 2010
Accepted Date: January 6, 2011
Published on Web Date: January 10, 2011

DOI: 10.1021/jz1015422 | J. Phys. Chem. Lett. 2011, 2, 176–184

Table 1. Advantages and Disadvantages of the Electrode Materials That Are Currently in Play

electrode material	cell voltage (V)	capacity (mA h/g)	specific energy (mW h/g)	advantages	disadvantages
layered $LiCoO_2$ cathode (2-d structure)	~4	140	560	high electronic and Li^+ ion conductivity; revolutionized the portable electronics market	expensive and toxic Co; safety concerns; only 50% of the theoretical capacity can be utilized
spinel $LiMn_2O_4$ cathode (3-d structure)	~4	120	480	inexpensive and environmentally benign Mn; high electronic and Li^+ ion conductivity; excellent rate capability; good safety	severe capacity fade at elevated temperatures (55 °C)
olivine $LiFePO_4$ cathode (1-d structure)	~3.5	160	560	inexpensive and environmentally benign Fe; covalently bonded PO_4 groups lead to excellent safety	low electronic and Li^+ ion conductivity; needs small particle size and carbon coating to realize high rate capability; high processing cost
graphite anode	~0.1	370	—	inexpensive and environmentally benign C; low operating potential maximizes cell voltage	SEI layer formation and lithium plating lead to safety concerns; high processing cost

to $0 \le x \le 0.5$.[2,3] In contrast, both the $Ni^{3+/4+}$ and the $Mn^{3+/4+}$ couples offer better safety and higher capacity than the $Co^{3+/4+}$ couple as the $Ni^{3+/4+}$:3d band barely touches the top of the O^{2-}:2p band while the $Mn^{3+/4+}$:3d band lies well above the top of the O^{2-}:2p band. As a consequence, layered solid solutions like the $LiNi_{1/3}Mn_{1/3}Co_{1/3}O_2$ cathode[4,5] are replacing $LiCoO_2$ in portable electronics due to batter safety and lower cost.

Because of the safety concerns and high cost, spinel $LiMn_2O_4$ and olivine $LiFePO_4$ have become appealing for transportation applications due to the low cost and environmental friendliness of Mn and Fe, good structural and chemical stabilities, and high charge−discharge rate capability. However, their limited energy is a drawback. Mn dissolution due to the disproportionation of Mn^{3+} into Mn^{4+} and Mn^{2+} is the major issue that has plagued spinel $LiMn_2O_4$ over the years,[6,7] but it could be suppressed significantly by cationic and anionic substitutions.[8,9] The substitution of lower-valent cations like Li^+ and Ni^{2+} for Mn^{3+} in $LiMn_2O_4$ increases the average oxidation state of Mn from 3.5+ to ~3.6+, which suppresses both Mn dissolution and dynamic Jahn−Teller distortion, resulting in significantly improved performance. The progress made with spinel $LiMn_2O_4$ by industry around the world has made it a leading candidate for vehicle applications such as the Chevy Volt. Often, the stabilized spinel cathode is blended with ~30 wt % of a layered oxide like $LiNi_{1/3}Mn_{1/3}Co_{1/3}O_2$ for these applications to increase the capacity and further reduce the total dissolved Mn content in the cell. On the other hand, the major issue with $LiFePO_4$ is the poor lithium ion and electronic conduction. These difficulties have been overcome by making $LiFePO_4$ as nanoparticles and coating the particles with conductive carbon.[10,11] As a result, $LiFePO_4$ has emerged as another leading candidate for vehicle applications. However, the $LiMn_2O_4$-based spinel cathodes offer significant cost advantages compared to the $LiFePO_4$ olivine cathodes due to the high processing cost associated with the manufacturing of carbon-coated nano-$LiFePO_4$.

While the operating voltage of graphite close to that of Li/Li^+ is attractive to maximize the cell energy, the lying of its electrochemical potential above the lowest unoccupied molecular orbital (LUMO) of the electrolyte, such as the $LiPF_6$ in 1:1 ethylene carbonate (EC)/diethyl carbonate (DEC) electrolyte, results in a reduction of the electrolyte on the graphite surface due to the transfer of electrons from the graphite anode to the LUMO of the organic solvents (EC and DEC) in the electrolyte[1] (Figure 2). This reaction leads to the formation of a solid−electrolyte interfacial (SEI) layer on the graphite surface. Although the SEI layer formed by this initial reaction acts as a barrier to further electron transfer from the anode to the electrolyte LUMO, the difficulty of lithium ion diffusion through the SEI layer results in a plating of metallic lithium on graphite, particularly at cold temperatures under the conditions of fast charge; the lithium plating followed by dendrite formation and internal short-circuiting through the separator can become a safety hazard. Although this is not a serious issue with small batteries used in portable devices, it can become deadly in the large cells necessary for transportation and stationary storage applications. Moreover, although the lithium ion diffusivity is high parallel to the graphene planes, the sluggish lithium ion diffusion perpendicular to the graphene plane and along grain boundaries degrades the rate capability of graphite.[12]

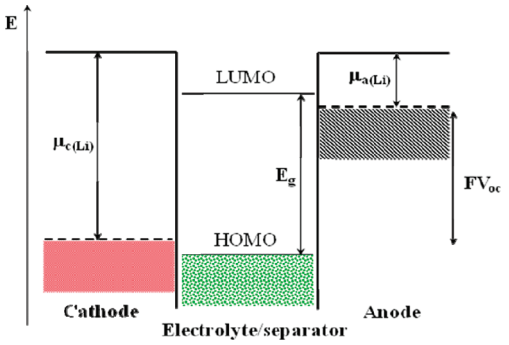

Figure 2. Schematic energy diagram of a lithium cell at open circuit. $\mu_{a(Li)}$ and $\mu_{c(Li)}$ refer, respectively, to the lithium chemical potential in the anode and cathode. E_g refers to the band gap in the electrolyte.

The drawbacks associated with the cathodes and anodes that are currently in play have prompted the development of

DOI: 10.1021/jz1015422 | J. Phys. Chem. Lett. 2011, 2, 176–184

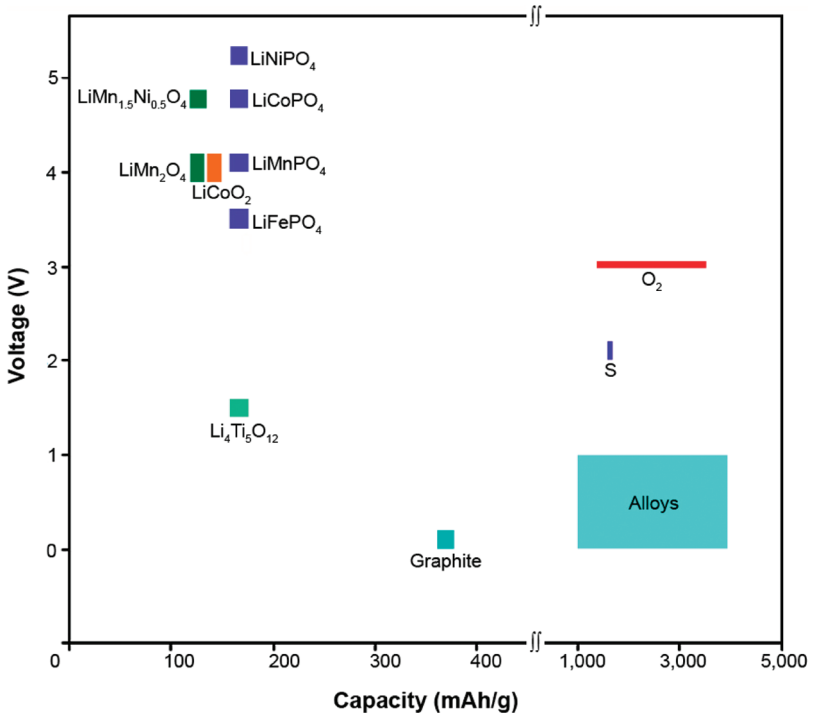

Figure 3. Voltage and capacity ranges of some cathode and anode materials.

alternate cathode and anode materials. There are several alternative cathode and anode materials possible, as seen in Figure 3, in terms of increasing the energy and power or lowering the cost or improving the safety. However, these alternatives also face several technological challenges, and the following sections focus on addressing these challenges and exploiting them for future-generation lithium ion cells.

High-Voltage, High-Capacity Cathode Materials. With a desire to increase the energy density, there is growing interest in cathodes that operate at higher voltages (> 4.2 V) and/or exhibit higher capacities. Figure 3 compares the voltage ranges and capacity values of several known cathode materials. Among them, spinel $LiMn_{1.5}Ni_{0.5}O_4$, olivine $LiCoPO_4$, and olivine $LiNiPO_4$, with operating voltages of, respectively, 4.7, 4.8, and 5.2 V, belong to the high-voltage cathode category. On the other hand, lithium-rich layered $Li[Li,Mn,Ni,Co]O_2$ and Li_2MSiO_4 (M = Mn, Fe, Co, and Ni) belong to the high-capacity category, although some of them also involve charging to a higher voltage of > 4.5 V to fully utilize their capacity.

The major difficulty in utilizing the high-voltage cathodes is the instability of the organic electrolytes, such as the $LiPF_6$ in 1:1 ethylene carbonate (EC)/diethyl carbonate (DEC) electrolyte, in contact with the cathode surface at the high operating voltages of > 4.5 V.

The major difficulty in utilizing the high-voltage cathodes is the instability of the organic electrolytes, such as the $LiPF_6$ in 1:1 ethylene carbonate (EC)/diethyl carbonate (DEC) electrolyte, in contact with the cathode surface at the high operating voltages of > 4.5 V. The lying of the cathode electrochemical potential below the highest occupied molecular orbital (HOMO) of such organic solvents leads to oxidation of the electrolyte on the cathode surface due to the transfer of electrons from the electrolyte HOMO to the cathode[1] (Figure 2), resulting in the formation of a SEI layer on the cathode surface, which becomes severe and aggressive particularly at elevated temperatures (~55 °C). These reactions degrade the electrolyte and cathode and result in capacity loss and lower Coulombic efficiency during cycling. Although such reactions could be suppressed to some extent by introducing a few percent of additives into the electrolyte solution, such a strategy may not be able to fully solve the problem. Alternatively, development of new electrolytes in which the HOMO lies well below the electrochemical potential of the cathode is being intensively pursued. However, the reactivity of the highly oxidizing cathode surface could still pose problems for long-term stability and cycle life with any of the electrolytes. One way to overcome this difficulty is to develop robust cathode surfaces that can provide good compatibility with the electrolytes and suppress SEI layer formation. Accordingly, the following sections focus on surface-modified high-voltage cathodes.

High-Voltage Spinel Cathodes. The $LiMn_{1.5}Ni_{0.5}O_4$ spinel with the $Ni^{2+/3+}$ and $Ni^{3+/4+}$ redox couples offers a capacity

DOI: 10.1021/jz1015422 | J. Phys. Chem. Lett. 2011, 2, 176–184

of ~130 mA h/g at a nearly flat voltage of ~4.7 V. With three-dimensional lithium ion diffusion, hopping electronic conduction across the shared MnO_6 octahedral edges, and a higher operating voltage of ~4.7 V, it is becoming an attractive candidate for high-power applications such as transportation and stationary storage. The major issues with this system are the formation of a $Ni_{1-x}Li_xO$ impurity phase and chemical instability in contact with the electrolyte at the high operating voltage. The $Ni_{1-x}Li_xO$ impurity phase could, however, be eliminated by a small amount of cationic substitutions for Ni or for both Ni and Mn as in $LiMn_{1.5}Ni_{0.42}Zn_{0.08}O_4$ and $LiMn_{1.42}Ni_{0.42}Co_{0.16}O_4$.[13] The cycle life and rate capability could, on the other hand, be improved significantly by surface modification of the cation-substituted $LiMn_{1.42}Ni_{0.42}Co_{0.16}O_4$ cathode with inert materials like $AlPO_4$, ZnO, Al_2O_3, and Bi_2O_3, as seen in Figure 4.[14] The coating protects the active cathode material surface from direct contact with the electrolyte and thereby suppresses the formation of thick SEI layers, as indicated by X-ray photoelectron spectroscopic (XPS) analysis. Moreover, the surface modification and suppression of SEI layer formation help to maintain the high rate capability as the cathodes are cycled compared to the unmodified cathode, resulting in better rate capability retention (Figure 4) during long-term cycling.

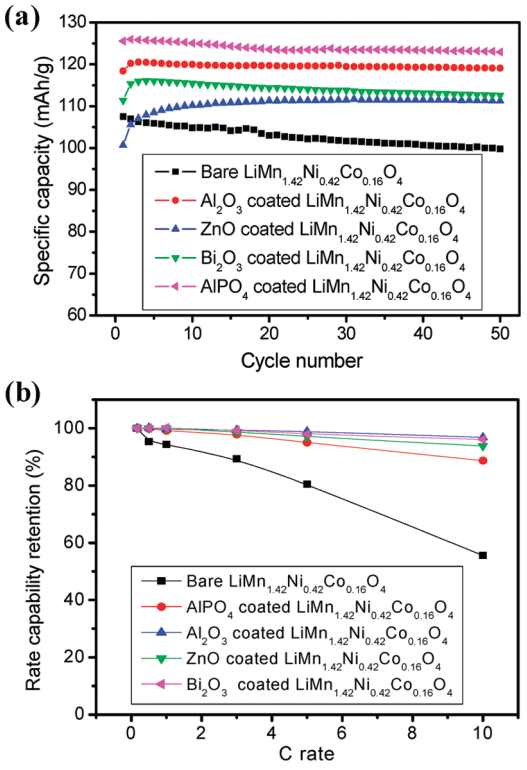

Figure 4. (a) Cycling performances and (b) rate capability retentions of bare and 2 wt % Al_2O_3-, ZnO-, Bi_2O_3-, and AlPO4-coated $LiMn_{1.42}Ni_{0.42}Co_{0.16}O_4$. The rate capability retention is defined as the ability to retain the rate capability upon cycling, and the rate capability retention values are calculated here as the percentage ratio of the rate capability measured after 50 cycles to that measured after 3 cycles. Reprinted from ref 14.

However, it may be difficult to obtain a uniform, robust coating of the cathode surface by postchemical processing of the already synthesized cathodes; it will also involve additional processing cost. Interestingly, certain cations like Fe^{3+}, Cr^{3+}, and Ga^{3+} self-segregate during the high-temperature synthesis and cooling process to the surface, which can offer better chemical stability in contact with the electrolyte.[15] For example, Figure 5 compares the cyclability and rate capability of $LiMn_{1.5}Ni_{0.5}O_4$ and the Fe-substituted samples. The $LiMn_{1.5}Ni_{0.42}Fe_{0.08}O_4$ sample with a small amount of Fe exhibits superior cyclability and rate capability compared to $LiMn_{1.5}Ni_{0.5}O_4$. Electrochemical impedance spectroscopic (EIS) data reveal that the Fe-substituted samples exhibit lower surface resistance and charge-transfer resistance compared to $LiMn_{1.5}Ni_{0.5}O_4$. An examination of the samples by XPS reveals that while the relative concentrations of the elements in the bulk are close to the nominal values, the surface of the Fe-substituted samples has a higher concentration of Fe and a lower concentration of Ni compared to those of the bulk. The enrichment of the surface by the catalytically less active Fe suppresses the formation of thick SEI layers and thereby lowers the impedance and enhances the electrochemical performance. The self-surface segregation was also confirmed recently by us with time-of-flight secondary ion mass spectroscopy (TOF-SIMS). More importantly, the self-surface

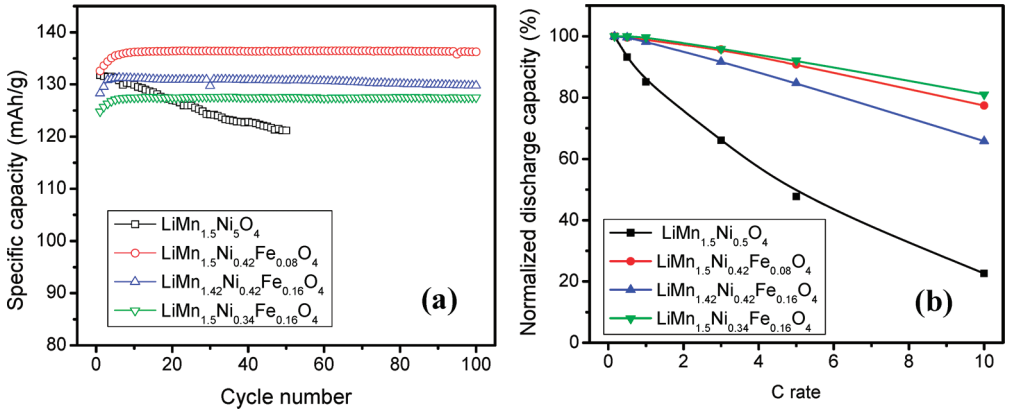

Figure 5. Comparison of the (a) cycling performances and (b) normalized discharge capacity at various C rates in reference to the value at the C/6 rate of $LiMn_{1.5}Ni_{0.5}O_4$ and the Fe-substituted samples. Reprinted from ref 15.

DOI: 10.1021/jz1015422 | J. Phys. Chem. Lett. 2011, 2, 176–184

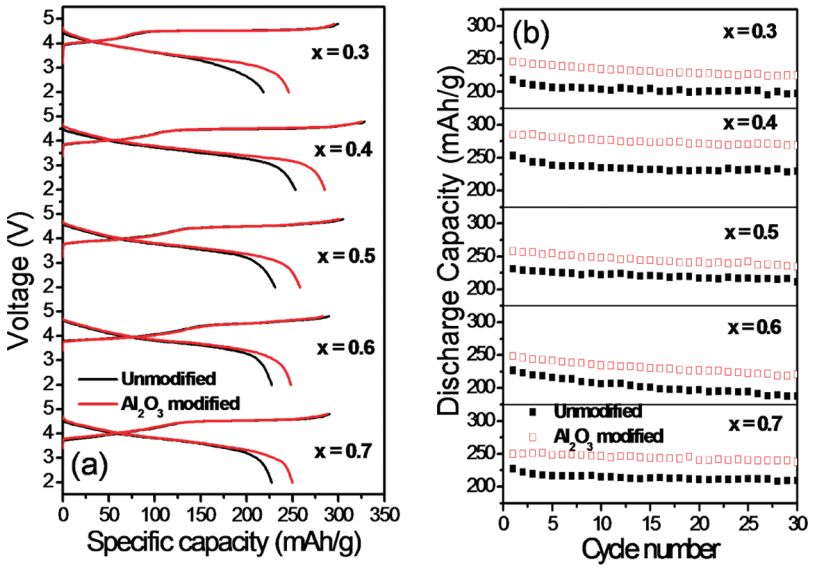

Figure 6. (a) First charge−discharge and (b) cycle life of pristine and Al_2O_3-coated $(1-x)Li[Li_{1/3}Mn_{2/3}O_2]-xLi[Mn_{1/3}Co_{1/3}Ni_{1/3}O_2]$.

segregated samples like $LiMn_{1.5}Ni_{0.42}Ga_{0.08}O_4$ exhibit superior capacity retention at elevated temperatures even with a conventional electrolyte like LiPF6 in EC/DEC without any additives. Thus, this type of self-surface segregation of robust cations during synthesis may be a cost-effective way to overcome the chemical instability of the cathode surface in contact with the electrolyte.

High-Capacity, High-Voltage Layered Oxide Cathodes. Lithium-excess layered oxides Li[Li,Mn,Ni,Co]O_2, which are solid solutions between layered $Li[Li_{1/3}Mn_{2/3}]O_2$ (commonly designated as Li_2MnO_3) and $LiMO_2$ (M = Ni, Co, Mn), have been found in recent years to offer much higher capacity values of ∼250 mA h/g compared to those of the layered $LiCoO_2$.[16−20] The high capacities of these oxides have been attributed to the irreversible loss of oxygen from the lattice during the first charge and the consequential lowering of the oxidation state of the transition-metal ions at the end of first discharge.[16,19] However, these high-capacity layered cathodes suffer from a huge irreversible capacity loss of 40−100 mA h/g in the first charge−discharge cycle and poor rate capability. The huge irreversible capacity loss has been attributed to the elimination of oxide ion and lithium ion vacancies from the layered lattice at the end of the first charge.[19] The poor rate capability could be related to the low electronic conductivity associated with the Mn^{4+} ions[21] and the thick SEI layer formed by a reaction of the cathode surface with the electrolyte.[22]

Interestingly, surface modification of the lithium-excess layered composition $Li[Li_{0.2}Mn_{0.54}Ni_{0.13}Co_{0.13}]O_2$ with nanostructured Al_2O_3, $AlPO_4$, or RuO_2 or their mixtures has been found to decrease the irreversible capacity loss and increase the discharge capacity (Figure 6).[22−27] The decrease in irreversible capacity loss upon surface modification compared to that for the unmodified sample has been attributed to the retention of a higher number of oxide ion and lithium ion vacancies in the layered lattice at the end of the first charge. More importantly, despite the coating with insulating materials like Al_2O_3 and $AlPO_4$, the surface-modified samples exhibit much higher rate capability than the unmodified sample.[26,27] EIS data reveal that the surface-modified samples exhibit lower charge-transfer resistance compared to the unmodified sample similar to that observed with the 5 V spinel.[14] An XPS analysis of the samples reveals that the higher rate capability of the surface-modified samples is due to the suppression of SEI layer formation.[27] Thus, development of robust cathode surfaces is an attractive strategy to overcome the instability of the high-voltage cathodes in contact with the liquid electrolytes and thereby improve the energy, power, and cycle life.

High-Voltage or High-Capacity Polyanion Cathodes. Intrigued by the success with nanostructured olivine $LiFePO_4$,[10,11] other olivines like $LiMnPO_4$, $LiCoPO_4$, and $LiNiPO_4$ have been pursued as they exhibit a much higher voltage of, respectively, 4.1, 4.8, and 5.2 V compared to 3.45 V for $LiFePO_4$.[28−30] However, it is hard to realize electrochemical performances comparable to that of $LiFePO_4$ with $LiMnPO_4$ and $LiCoPO_4$, while $LiNiPO_4$ is difficult to evaluate due to the electrolyte instability at the high operating voltage of 5.2 V.[31−33] Interestingly, the substitution of small amounts of Fe for Mn or Co in $LiMn_{1-x}Fe_xPO_4$ and $LiCo_{1-x}Fe_xPO_4$ has been found to improve the capacity and cycle life significantly.[34−36] The better performance of the Fe-substituted solid solutions could be related to the suppression of Jahn−Teller distortion and Mn dissolution in $LiMn_{1-x}Fe_xPO_4$ as well as the self-surface segregation of Fe in both $LiMn_{1-x}Fe_xPO_4$ and $LiCo_{1-x}Fe_xPO_4$, similar to that found with the 4.8 V spinel $LiMn_{1.5}Ni_{0.42}Fe_{0.08}O_4$.[15] Thus, with the high-voltage olivines, only the solid solutions appear to be viable candidates, but they have the drawback of steps in the voltage profiles.

While the $LiMPO_4$ cathodes offer capacity corresponding to the reversible extraction of one lithium ion per formula unit, Li_2MSiO_4 (M = Mn, Fe, Co, and Ni) cathodes offer the possibility of reversibly extracting/inserting two lithium ions per formula unit with a theoretical capacity of ∼330 mA h/g. However, only limited literature is available on this class of materials due to the difficulty in synthesizing phase-pure Li_2MSiO_4 samples,

DOI: 10.1021/jz1015422 | J. Phys. Chem. Lett. 2011, 2, 176–184

and they suffer from poor electronic conductivity like the olivine phosphates. Interestingly, Li_2FeSiO_4 and Li_2MnSiO_4 could recently be synthesized by a microwave–solvothermal process at 300 °C for 20 min, followed by heating at 650 °C for 6 h in an Ar atmosphere to obtain well-crystalline samples with carbon coating.[37] The Li_2FeSiO_4 thus obtained delivered a discharge capacity of 148 and 204 mA h/g, respectively, at room temperature and 55 °C, while Li_2MnSiO_4 delivered 210 and 250 mA h/g, respectively, at room temperature and 55 °C, indicating the extraction of more than one lithium ion. However, while Li_2FeSiO_4 exhibited excellent cycle life, Li_2MnSiO_4 exhibited poor cycle life.

High-Capacity Sulfur and Oxygen Cathodes. Sulfur and oxygen offer enormous theoretical capacities of, respectively, 1675 mA h/g at an average operating voltage of 2.1 V and 3350 mA h/g at an operating voltage of ~3 V, which are an order of magnitude higher than that realized with the insertion compound cathodes discussed above (Figure 3). The discharge–charge process of the sulfur cathode with the metallic lithium anode involves the formation of a series of products, Li_2S_8, Li_2S_4, Li_2S_2, and Li_2S. Among them, only Li_2S_2 and Li_2S are insoluble in the electrolyte, and both of the polysulfide ions Li_2S_8 and Li_2S_4 formed at the beginning of the discharge process are soluble in the electrolyte. The major issues with the sulfur cathode are the migration of the dissolved polysulfide ions S_8^{2-} and S_4^{2-} toward the lithium anode and the high resistivity (2×10^{15} Ω m) of S. The dissolution and redeposition of the various reaction species result in the deposition of highly resistive layers on both of the electrodes and loss of active material during the charge–discharge process, resulting in severe capacity fade during cycling.[38] Several approaches, such as adding nanostructured carbon, replacing binders, mixing electrolytes, and employing sulfur composites (e.g., mesoporous carbon nanofibers filled with amorphous sulfur), have been pursued to overcome this problem, and they have led to some success.[39] Further work is necessary to realize acceptable cycle life and to employ them in commercial cells. Development of electrolytes in which the polysulfide ions are insoluble can greatly help.

The huge capacity of O_2 and the abundance of oxygen in air make the lithium–O_2 battery appealing. Although the concept of a rechargeable lithium–O_2 battery has been known for some time,[40,41] it has received an explosion of interest since 2009.[42] The discharge–charge process of the oxygen cathode with a metallic lithium anode involves the formation of a series of products, superoxide (LiO_2), peroxide (Li_2O_2), and oxide (Li_2O). The major issues with the lithium–O_2 batteries are the lack of efficient electrocatalysts and air cathodes both for the oxygen reduction reaction (ORR) and oxygen evolution reaction (OER), the challenge to keep the electrolyte and lithium metal from the attack of H_2O and CO_2 from the ambient air, and the safety concerns and poor cycle life of the metallic lithium anode. In addition, the high reactivity of the superoxide ions formed during discharge causes a severe degradation of the electrolyte. These challenges are formidable, and a fundamental understanding of the electrochemical reactions occurring in aprotic solvents could help to develop new electrolytes and electrocatalysts that avoid the formation of superoxide ions and offer fast ORR and OER kinetics. For more details, the readers can refer to another Perspective article.[42]

High-Capacity Anode Materials. The limited capacity (372 mA h/g) of the currently used graphite anode and the possibility of lithium plating and safety hazards arising from an operating voltage close to that of Li/Li^+ have prompted interest in alternative anodes. $Li_4Ti_5O_{12}$ with the spinel structure has emerged as an attractive alternative as its higher operating voltage of 1.5 V versus Li/Li^+ prevents SEI layer formation with the electrolyte and offers excellent safety.[43,44] However, its limited capacity of 175 mA h/g along with the higher operating voltage sacrifices the cell voltage and energy significantly.

In this regard, several lithium alloy anode materials Li_xM_y have attracted much attention due to their high capacity values, $Li_{3.75}Si$ (3578 mA h/g),[45] $Li_{3.75}Ge$ (1385 mA h/g),[46] $Li_{4.4}Sn$ (993 mA h/g),[47] and Li_3Sb (660 mA h/g).[48] Also, an operating voltage well above that of Li/Li^+ with some of them can avoid lithium plating, significantly enhancing the safety. The major issue with the alloy anodes is the severe capacity fade, arising from a huge volume change occurring during the charge–discharge (lithium alloying/dealloying) process. The volume change leads to lattice stress and consequential cracking and crumbling of the alloy particles during cycling, resulting in abrupt loss in capacity within a few charge–discharge cycles.

To overcome the above problem, an active–inactive composite strategy involving a mixture of two materials, one reacting with lithium and the other acting as an electrochemically inactive matrix to buffer the volume change during the charge–discharge cycling, has been pursued. For example, Sn–M–C systems with M = Ti, V, Cr, Mn, Fe, and Co have been pursued with this strategy,[49] and Sony Corporation has introduced a new lithium ion battery called Nexelion with an amorphous Sn–Co–C composite as the anode.[50] However, this strategy was not successful with any other Sn–M–C systems, and the high cost of Co prohibits the adoption of Sn–Co–C in large cells for vehicle and stationary storage applications. Clearly, design of safe, low-cost alternatives is critical for these emerging applications.

We recently showed that Sb–MO_x–C (M = Al, Ti, or Mo) nanocomposites synthesized by a mechanochemical reduction of Sb_2O_3 with Al, Ti, or Mo in the presence of acetylene black exhibit excellent cycle life with a capacity of 500 mA h/g at an average operating voltage of 1.0 V (Figure 7).[51] A homogeneous dispersion of 15–20 nm Sb particles in the conductive, amorphous MO_x–C matrix and the buffering of the volume expansion by the MO_x–C ceramic matrix lead to good cycle life (Figure 8). These nanocomposites have a tap density of 1.5 g/cm^3 at this early stage compared to ~1 g/cm^3 for commercial graphite, offering a significant advantage in volumetric capacity. Moreover, these nanocomposites are produced with inexpensive raw materials and ambient-temperature mechanical milling, offering significant cost advantages. Although the operating voltage sacrifices some cell energy compared to graphite, it offers much better safety. Sn–TiC–C nanocomposites obtained by a similar approach in which the TiC–C matrix buffers the volume expansion have also been found to exhibit good cycle life.[52]

DOI: 10.1021/jz1015422 | J. Phys. Chem. Lett. 2011, 2, 176–184

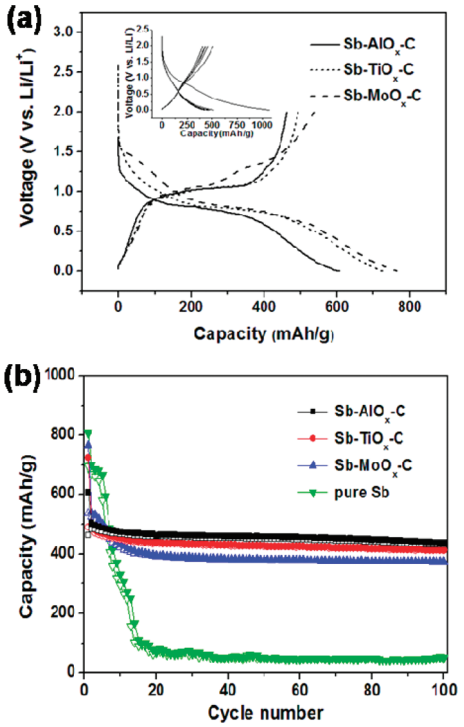

Figure 7. Comparison of the (a) charge−discharge profiles and (b) cycling performances of Sb−MO_x−C (M = Al, Ti, and Mo) nanocomposites. Reprinted from ref 51.

Considerable effort is being paid to manipulating the nanostructure of Si to overcome the difficulties associated with its huge volume change of ~400 % as it exhibits a huge capacity of ~4000 mA h/g. For example, Si nanowire architectures as well as nanocomposites such as Si/C and Si/TiB_2 have been found to show good cyclability.[53,54]

Nanostructured oxides MO_x undergoing displacement reactions with lithium to form metal M nanoparticles in the Li_2O matrix have also been found to exhibit high capacities of ~1000 mA h/g.[55−57] Although high capacities with good cyclability could be achieved with carbon-coated oxide nanostructures, these displacement reactions tend to exhibit significant differences in the charge and discharge voltages, which is a drawback.

Overall, lithium ion batteries are promising for transportation and stationary electrical energy storage. Reaction of the cathode surface with the electrolyte is a major challenge with the high-voltage layered, spinel, olivine, and silicate cathodes, but they could be minimized in some cases by postchemical surface modification or self-segregation of certain robust cations to the surface during the synthesis process. Such surface decoration improves the cycle life and charge−discharge rate capability due to the suppression of the formation of thick SEI layers. The use of lithium-free S and O_2 as cathodes has the challenge of overcoming the safety problems of the metallic lithium anode in addition to the dissolution of polysulfide ions and the poor oxygen reduction and oxygen evolution reaction kinetics. While the confinement of the polysulfide ions within the electrode structure or the development of new electrolytes in which the polysulfide ions are insoluble can benefit the

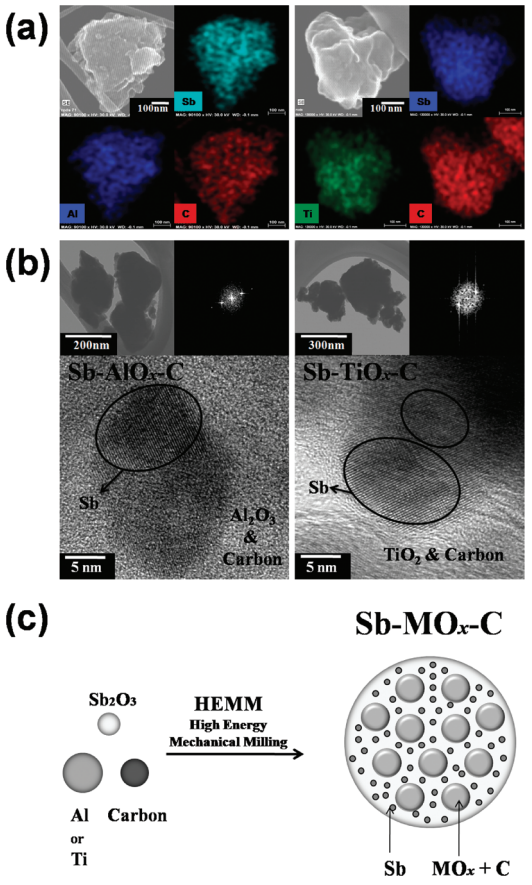

Figure 8. (a) Scanning transmission electron microscopy (STEM) images, (b) high-resolution transmission electron microscopy (HR-TEM) images, and (c) schematic description of the Sb−MO_x−C (M = Al, Ti, and Mo) nanocomposites. Reprinted from ref 51.

lithium−sulfur cells, development of efficient ORR and OER electrocatalysts is critical for the lithium−air cells. Huge volume expansion is the major challenge with the high-capacity alloy anodes, and nanoengineered active−inactive composites could alleviate the volume expansion and offer good cycle life. Development of new high-voltage electrolytes with a wide electrochemical window (0−5.3 V versus Li/Li^+) to be

Development of advanced materials and electrode characterization tools and methodologies coupled with computational modeling and simulation can help to enhance the fundamental understanding of the chemical and physical processes occurring.[12,60]

DOI: 10.1021/jz1015422 | J. Phys. Chem. Lett. 2011, 2, 176–184

compatible with both the cathode and anode will have a significant impact in the field. In addition, development of new low-cost, safe, high energy density cathodes and anodes (lithium-free and lithium-containing) including inorganic, organic,[58] and metal−organic framework[59] materials, as well as novel synthesis and processing approaches can help meet the challenges of the requirements for transportation and stationary storage applications. Finally, development of advanced materials and electrode characterization tools and methodologies coupled with computational modeling and simulation can help to enhance the fundamental understanding of the chemical and physical processes occurring.[12,60]

AUTHOR INFORMATION

Corresponding Author:

*Tel.: +1 512 471 1791. Fax: +1 512 471 7681. E-mail: rmanth@mail.utexas.edu.

Biographies

Arumugam Manthiram is a Professor and holder of the Joe C. Walter Chair in Engineering in the Materials Science and Engineering Graduate Program and Department of Mechanical Engineering at The University of Texas at Austin. His research interests are in the area of materials for lithium ion batteries, fuel cells, and solar cells, including novel synthesis approaches for nanomaterials. He has authored 400 publications including more than 320 journal articles. See www.me.utexas.edu/~manthiram for further details.

ACKNOWLEDGMENT This research described herein was supported by the U.S. Department of Energy Contract No. DE-AC02-05CH1123, NASA Glenn Research Center, and Welch Foundation Grant F-1254. I am grateful to my students and postdoctoral researchers for contributing to our battery research.

REFERENCES

(1) Goodenough, J. B.; Kim, Y. Challenges of Rechargeable Lithium Batteries. *Chem. Mater.* **2010,** *22*, 587–603.

(2) Chebiam, R. V.; Kannan, A. M.; Prado, F.; Manthiram, A. Comparison of the Chemical Stability of High Energy Density Cathodes of Lithium-Ion Batteries. *Electrochem. Commun.* **2001,** *3*, 624–627.

(3) Choi, J.; Alvarez, E.; Arunkumar, T. A.; Manthiram, A. Proton Insertion into Oxide Cathodes During Chemical Delithiation. *Electrochem. Solid-State Lett.* **2006,** *9*, A241–A244.

(4) Ohzuku, T.; Makimura, Y. Layered Lithium Insertion Material of $LiCo_{1/3}Ni_{1/3}Mn_{1/3}O_2$ for Lithium-Ion Batteries. *Chem. Lett.* **2001,** *30*, 642–643.

(5) Lu, Z.; MacNeil, D. D.; Dahn, J. R. Layered $Li[Ni_xCo_{1-2x}Mn_x]O_2$ Cathode Materials for Lithium-Ion Batteries. *Electrochem. Solid-State Lett.* **2001,** *4*, A200–A203.

(6) Gummow, R. J.; de Kock, A.; Thackeray, M. M. Improved Capacity Retention in Rechargeable 4 V Lithium/Lithium-Manganese Oxide (Spinel) Cells. *Solid State Ionics.* **1994,** *69*, 59–67.

(7) Jang, D. H.; Shin, Y. J.; Oh, S. M. Dissolution of Spinel Oxides and Capacity Losses in 4 V $Li/Li_xMn_2O_4$ Cells. *J. Electrochem. Soc.* **1996,** *143*, 2204–2211.

(8) Shin, Y.; Manthiram, A. Factors Influencing the Capacity Fade of Spinel Lithium Manganese Oxides. *J. Electrochem. Soc.* **2004,** *151*, A204–A208.

(9) Choi, W.; Manthiram, A. Superior Capacity Retention Spinel Oxyfluoride Cathodes for Lithium Ion Batteries. *Electrochem. Solid-State Lett.* **2006,** *9*, A245–A248.

(10) Chung, S.-Y.; Bloking, J. T.; Chiang, Y.-M. Electronically Conductive Phospho-olivines as Lithium Storage Electrodes. *Nat. Mater.* **2002,** *1*, 123–128.

(11) Ellis, B.; Kan, W. H.; Makahnouk, W. R. M.; Nazar, L. F. Synthesis of Nanocrystals and Morphology Control of Hydrothermally Prepared $LiFePO_4$. *J. Mater. Chem.* **2007,** *17*, 3248–3254.

(12) Persson, K.; Sethuraman, V. A.; Hardwick, L. J.; Hinuma, Y.; Meng, Y. S.; Van der Ven, A.; Srinivasan, V.; Kostecki, R.; Ceder, G. Lithium Diffusion in Graphitic Carbon. *J. Phys. Chem. Lett.* **2010,** *1*, 1176–1180.

(13) Arunkumar, T. A.; Manthiram, A. Influence of Lattice Parameter Differences on the Electrochemical Performance of the 5 V Spinel $LiMn_{1.5-y}Ni_{0.5-z}M_{y+z}O_4$ (M = Li, Mg, Fe, Co, and Zn). *Electrochem. Solid-State Lett.* **2005,** *8*, A403–A405.

(14) Liu, J.; Manthiram, A. Understanding the Improvement in the Electrochemical Properties of Surface Modified 5 V $LiMn_{1.42}Ni_{0.42}Co_{0.16}O_4$ Spinel Cathodes in Lithium-Ion Cells. *Chem. Mater.* **2009,** *21*, 1695–1707.

(15) Liu, J.; Manthiram, A. Understanding the Improved Electrochemical Performances of Fe-Substituted 5 V Spinel Cathode $LiMn_{1.5}Ni_{0.5}O_4$. *J. Phys. Chem. C* **2009,** *113*, 15073–15079.

(16) Lu, Z.; Beaulieu, L. Y.; Donaberger, R. A.; Thomas, C. L.; Dahn, J. R. Synthesis, Structure, and Electrochemical Behavior of $Li[Ni_xLi_{1/3-2x/3}Mn_{1/3-2x/3}]O_2$. *J. Electrochem. Soc.* **2002,** *149*, A778–A791.

(17) Lu, Z.; Dahn, J. R. Understanding the Anomalous Capacity of $Li/Li[Ni_xLi_{(1/3-2x/3)}Mn_{(2/3-x/3)}]O_2$ Cells Using In Situ X-Ray Diffraction and Electrochemical Studies. *J. Electrochem. Soc.* **2002,** *149*, A815–A822.

(18) Kang, S.-H.; Sun, Y. K.; Amine, K. Electrochemical and Ex Situ X-Ray Study of $Li(Li_{0.2}Ni_{0.2}Mn_{0.6})O_2$ Cathode Material for Li Secondary Batteries. *Electrochem. Solid-State Lett.* **2003,** *6*, A183–A186.

(19) Armstrong, A. R.; Holzapfel, M.; Novák, P.; Johnson, C. S.; Kang, S.-H.; Thackeray, M. M.; Bruce, P. G. Demonstrating Oxygen Loss and Associated Structural Reorganization in the Lithium Battery Cathode $Li[Ni_{0.2}Li_{0.2}Mn_{0.6}]O_2$. *J. Am. Chem. Soc.* **2006,** *128*, 8694–8698.

(20) Arunkumar, T. A.; Wu, Y.; Manthiram, A. Factors Influencing the Irreversible Oxygen Loss and Reversible Capacity in Layered $Li[Li_{1/3}Mn_{2/3}]O_2$-$Li[M]O_2$ (M = $Mn_{0.5-y}Ni_{0.5-y}Co_{2y}$ and $Ni_{1-y}Co_y$) Solid Solutions. *Chem. Mater.* **2007,** *19*, 3067–3073.

(21) Thackeray, M. M.; Kang, S.-H.; Johnson, C. S.; Vaughey, J. T.; Benedek, R.; Hackney, S. A. Li_2MnO_3-Stabilized $LiMO_2$ (M = Mn, Ni, Co) Electrodes for Lithium-Ion Batteries. *J. Mater. Chem.* **2007,** *17*, 3112–3125.

(22) Liu, J.; Manthiram, A. Understanding the Improvement in the Electrochemical Properties of Surface Modified 5 V $LiMn_{1.42}Ni_{0.42}Co_{0.16}O_4$ Spinel Cathodes in Lithium-Ion Cells. *Chem. Mater.* **2009,** *21*, 1695–1707.

(23) Wu, Y.; Manthiram, A. High Capacity, Surface-Modified Layered $Li[Li_{(1-x)/3}Mn_{(2-x)/3}Ni_{x/3}Co_{x/3}]O_2$ Cathodes with Low Irreversible Capacity Loss. *Electrochem. Solid-State Lett.* **2006,** *9*, A221–A224.

(24) Wu, Y.; Vadivel Murgan, A.; Manthiram, A. Surface Modification of High Capacity Layered $Li[Li_{0.2}Mn_{0.54}Ni_{0.13}Co_{0.13}]O_2$ Cathodes by $AlPO_4$. *J. Electrochem. Soc.* **2008,** *155*, A635–A641.

(25) Wu, Y.; Manthiram, A. Effect of Surface Modifications on the Layered Solid Solution Cathodes $(1-z)Li[Li_{1/3}Mn_{2/3}]O_2-(z)Li[Mn_{0.5-y}Ni_{0.5-y}Co_{2y}]O_2$. *Solid State Ionics* **2009,** *180*, 50–56.

(26) Wang, Q. Y.; Liu, J.; Vadivel Murugan, A.; Manthiram, A. High Capacity Double-Layer Surface Modified $Li[Li_{0.2}Mn_{0.54}Ni_{0.13}Co_{0.13}]O_2$ Cathode with Improved Rate Capability. *J. Mater. Chem.* **2009,** *19*, 4965–4972.

(27) Liu, J.; Manthiram, A. Functional Surface Modifications of High Capacity Layered $Li[Li_{0.2}Mn_{0.54}Ni_{0.13}Co_{0.13}]O_2$ Cathode. *J. Mater. Chem.* **2010,** *20*, 3961–3967.

(28) Padhi, A. K.; Nanjundasawamy, K. S.; Goodenough, J. B. Phospho-olivines as Positive-Electrode Materials for Rechargeable Lithium Batteries. *J. Electrochem. Soc.* **1997,** *144*, 1188–1194.

(29) Yang, J.; Xu, J. J. Synthesis and Characterization of Carbon-Coated Lithium Transition Metal Phosphates $LiMPO_4$ (M = Fe, Mn, Co, Ni) Prepared via a Nonaqueous Sol−Gel Route. *J. Electrochem. Soc.* **2006,** *153*, A716.

(30) Manthiram, A.; A. Vadivel Murugan, A.; Sarkar, A.; Muraliganth, T. Nanostructured Materials for Electrochemical Energy Storage and Conversion. *Ener. Environ. Sci.* **2008,** *1*, 621–638.

(31) Delacourt, C.; Poizot, P.; Morcrette, M.; Tarascon, J.-M.; Masquelier, C. One-Step Low-Temperature Route for the Preparation of Electrochemically Active $LiMnPO_4$ Powders. *Chem. Mater.* **2004,** *16*, 93–99.

(32) Bramnik, N. N.; Nikolowski, K.; Balhtz., C.; Bramnik, K. G.; Ehrenberg, H. Phase Transitions Occurring upon Lithium Insertion−Extraction of $LiCoPO_4$. *Chem. Mater.* **2007,** *19*, 908–915.

(33) Vadivel Murugan, A.; Muraliganth, T.; Ferreira, P. J.; Manthiram, A. Dimensionally Modulated, Single-Crystalline $LiMPO_4$ (M = Mn, Fe, Co, and Ni) with Nano Thumb-like Shapes for High Power Energy Storage. *Inorg. Chem.* **2009,** *48*, 946–952.

(34) Yamada, A.; Takei, Y.; Koizumi, H.; Sonoyama, N.; Kanno, R. Electrochemical, Magnetic, and Structural Investigation of the $Li_x(Mn_yFe_{1-y})PO_4$ Olivine Phases. *Chem. Mater.* **2006,** *18*, 804–813.

(35) Zaghib, K.; Mauger, A.; Gendron, F.; Massot, M.; Julien, C. M. Insertion Properties of $LiFe_{0.5}Mn_{0.5}PO_4$ Electrode Materials for Li-Ion Batteries. *Ionics* **2008,** *14*, 371–376.

(36) Muraliganth, T.; Manthiram, A. Understanding the Shifts in the Redox Potentials of Olivine $LiM_{1-y}M_yPO_4$ (M = Fe, Mn, Co, and Mg) Solid Solution Cathodes. *J. Phys. Chem. C.* **2010,** *114*, 15530–15540.

(37) Muraliganth, T.; Stroukoff, K. R.; Manthiram, A. Microwave-Solvothermal Synthesis of Nanostructured Li_2MSiO_4/C (M = Mn and Fe) Cathodes for Lithium-Ion Batteries. *Chem. Mater.* **2010,** *22*, 5754–5761.

(38) Cheon, S.-E.; Choi, S.-S.; Han, J.-S.; Choi, Y.-S.; Jung, B.-H.; Lim, H. S. Capacity Fading Mechanisms on Cycling a High-Capacity Secondary Sulfur Cathode. *J. Electrochem. Soc.* **2004,** *151*, A2067–A2073.

(39) Ji, X; Lee, K. T.; Nazar, L. F. A Highly Ordered Nanostructured Carbon−Sulphur Cathode for Lithium−Sulphur Batteries. *Nat. Mater.* **2009,** *8*, 500–506.

(40) Abraham, K. M.; Jiang, Z. A Polymer Electrolyte-Based Rechargeable Lithium/Oxygen Battery. *J. Electrochem. Soc.* **1996,** *143*, 1–5.

(41) Ogasawara, T.; Débart, A.; Holzapfel, M.; Novák, P.; Bruce, P. G. Rechargeable Li_2O_2 Electrode for Lithium Batteries. *J. Am. Chem. Soc.* **2006,** *128*, 1390–1393.

(42) Girishkumar, G.; McCloskey, B.; Luntz, A. C.; Swanson, S.; Wilcke, W. Lithium−Air Battery: Promise and Challenges. *J. Phys. Chem. Lett.* **2010,** *1*, 2193–2203.

(43) Ferg, E.; Gummow, R. J.; de Kock, A.; Thackeray, M. M. Spinel Anodes for Lithium-Ion Batteries. *J. Electrochem. Soc.* **1994,** *141*, L147–L150.

(44) Reale, P.; Panero, S.; Scrosati, B.; Garche, J.; Wohlfahrt-Mehrens, M.; Wachtler, M. A Safe, Low-Cost, and Sustainable Lithium-Ion Polymer Battery. *J. Electrochem. Soc.* **2004,** *151*, A2138–A2142.

(45) Ng, S.-H.; Wang, J.; Wexler, D.; Konstantinov, K.; Guo, Z.-P.; Liu, H.-K. Highly Reversible Lithium Storage in Spheroidal Carbon-Coated Silicon Nanocomposites as Anodes for Lithium-Ion Batteries. *Angew. Chem., Int. Ed.* **2006,** *45*, 6896–6899.

(46) Yoon, S; Park, C.-M.; Sohn, H.-J. Electrochemical Characterizations of Germanium and Carbon-Coated Germanium Composite Anode for Lithium-Ion Batteries. *Electrochem. Solid-State Lett.* **2008,** *11*, A42–A45.

(47) Idota, Y.; Kubota, T; Matsufuji, A.; Maekawa, Y.; Miyasaka, T. Tin-based Amorphous Oxide: A High-Capacity Lithium-Ion-Storage Material. *Science* **1997,** *276*, 1395–1398.

(48) Yang, J.; Takeda, Y.; Imanish, N.; Yamamoto, O. Ultrafine Sn and $SnSb_{0.14}$ Powders for Lithium Storage Matrices in Lithium-Ion Batteries. *J. Electrochem. Soc.* **1999,** *146*, 4009–4013.

(49) Todd, A. D. W.; Mar, R. E.; Dahn, J. R. Combinatorial Study of Tin−Transition Metal Alloys as Negative Electrodes for Lithium-Ion Batteries. *J. Electrochem. Soc.* **2006,** *153*, A1998–A2005.

(50) Mizutani, S.; Inoue, H. Negative Active Material and Method for Production Thereof, Non-aqueous Electrolyte Secondary Cell Using the Same. *U.S. Pat. Appl.*, N. 0208378, 2005.

(51) Yoon, S.; Manthiram, A. Sb−MO_x−C (M = Al, Ti, or Mo) Nanocomposite Anodes for Lithium Ion Batteries. *Chem. Mater.* **2009,** *21*, 3898–3904.

(52) Yoon, S.; Manthiram, A. Nanoengineered Sn−TiC−C Anode for Lithium Ion Batteries. *J. Mater. Chem.* **2010,** *20*, 236–239.

(53) Chan, C. K.; Peng, H.; Liu, G.; McIlwrath, K.; Zhang, X. F.; Huggins, R. A.; Cui, Y. High-Performance Lithium Battery Anodes Using Silicon Nanowires. *Nat. Nanotech.* **2008,** *3*, 31–35.

(54) Kim, H.; Cho, J. Superior Lithium Electroactive Mesoporous Si@Carbon Core−Shell Nanowires for Lithium Battery Anode Material. *Nano Lett.* **2008,** *8*, 3688–3691.

(55) Poizot, P.; Laruelle, S.; Grugeon, S.; Dupont, L.; Tarascon, J.-M. Nano-Sized Transition Metal Oxides as Negative Electrode Material for Lithium-Ion Batteries. *Nature* **2000,** *407*, 496–499.

(56) Taberna, P. L.; Mitra, S.; Poizot, P.; Simon, P.; Tarascon, J.-M. High Rate Capabilities Fe_3O_4-based Cu Nano-Architectured Electrodes for Lithium-ion Battery Applications. *Nat. Mater.* **2006,** *5*, 567–573.

(57) Muraliganth, T.; Vadivel Murugan, A.; Manthiram, A. Facile Synthesis of Carbon-Decorated Single-Crystalline Fe_3O_4 Nanowires and Their Application as High Performance Anode in Lithium Ion Batteries. *Chem. Commun.* **2009,** *49*, 7360–7362.

(58) Armand, M.; Grugeon, S.; Vezlin, H.; Laruelle, S.; Ribiere, P.; Poizot, P.; Tarascon, J.-M. Conjugated Dicarboxylate Anodes for Li-Ion Batteries. *Nat. Mater.* **2009,** *8*, 120–125.

(59) Okubo, M.; Asakura, D.; Mizuno, Y.; Kim, J.-D.; Mizokawa, T.; KUdo, T.; Honma, I. Switching Redox-Active Sites by Tautomerism in Prussian Blue Analogues $A_xMn_y[Fe(CN)_6]\cdot nH_2O$ (A: K, Rb): Robust Framework for Reversible Li Storage. *J. Phys. Chem. Lett.* **2010,** *1*, 2063–2071.

(60) Liu, J.; Kunz, M.; Chen, K.; Tamura, N.; Richardson, T. J. Visualization of Charge Distribution in a Lithium Battery Electrode. *J. Phys. Chem. Lett.* **2010,** *1*, 2120–2123.

DOI: 10.1021/jz1015422 | *J. Phys. Chem. Lett.* **2011,** *2*, 176–184